Journal of the European Ceramic Society 20 (2000) 2069–2077

Cation transport in yttria stabilized cubic zirconia: ^{96}Zr tracer diffusion in $(Zr_xY_{1-x})O_{2-x/2}$ single crystals with $0.15 \leqslant x \leqslant 0.48$

M. Kilo [a,*], G. Borchardt [a], B. Lesage [b], O. Kaïtasov [c], S. Weber [d], S. Scherrer [d]

[a] *Institut für Metallurgie, AG Thermochemie und Mikrokinetik, Technische Universität Clausthal, D-38678 Clausthal-Zellerfeld, Germany*
[b] *L.E.M.H.E., Bât. 410, Université Paris-Sud, F-91405 Orsay Cedex, France*
[c] *C.S.N.S.M., Bât. 108, Université Paris-Sud, F-91405 Orsay Cedex, France*
[d] *Laboratoire de Physique des Matériaux, Ecole des Mines de Nancy, F-54042 Nancy Cedex, France*

Dedicated to Professor Jean Philibert on the occasion of his 70th birthday.

Received 10 March 1999; received in revised form 19 February 2000; accepted 22 February 2000

Abstract

For a wide range of stabilizer concentrations in yttria stabilized cubic zirconia (YSZ), Zr diffusion data extracted from published creep data and dislocation loop shrinkage data are discussed together with published Zr tracer diffusion data and our own data on Zr tracer diffusion in order to identify the most probable point defect responsible for Zr diffusion. From this evaluation, complex defects can be ruled out, as the single vacancy, $V_{Zr}^{4'}$, fits best. © 2000 Elsevier Science Ltd. All rights reserved.

Keywords: Defects; Diffusion; Fuel cells; Vacancies; ZrO_2

1. Introduction

Lower valence cations like Y^{3+} or Ca^{2+} on Zr^{4+} sites introduce oxygen vacancies in zirconia and enlarge the stability range of the cubic phase in the concentration–temperature space down to low temperatures.[1] This feature makes it an oxygen ion conductor of prime interest for technical applications in solid oxide fuel cells. While oxygen transport has been intensively studied,[2] information on cation diffusion is fairly scarce. On the other hand, in the oxides with fluorite structure the slow cation diffusion governs diffusion creep and long-term ageing of the electrical (anionic) conductivity.[3] For yttria stabilized cubic zirconia (YSZ) there are only four data sets available on zirconium diffusion which were obtained via quite different experimental approaches:

- Interdiffusion experiments: Oishi et al.[4] determined zirconium diffusivities from zirconium–hafnium counter diffusion profiles in 16 mol% yttria containing YSZ–YSZ(+ hafnia) couples.
- Tracer diffusion: Solmon et al.[5] and Solmon[6] measured ^{96}Zr tracer diffusion in YSZ doped with 9.5, 11 and 18 mol% Y_2O_3, respectively.
- Dislocation loop annealing: Chien and Heuer[7] derived zirconium diffusivities from the variation of dislocation loop radii with time as measured by transmission electron microscopy (TEM) for two different stabilizer contents (9.4 and 18 mol% Y_2O_3, respectively).
- From creep measurements Dimos and Kohlstedt[8] and Gómez-García et al.[9] determined "effective cation lattice diffusivities".

In Table 1, the pertinent information is summarized for comparison. Fig. 1 shows the temperature dependence of the zirconium diffusivity with the atomic fraction of yttrium ions (on the cation sublattice) as a parameter. As can be seen from this diagram there are striking differences as to the variation of the zirconium diffusivity with stabilizer content, whereas the differences of the activation energies are less pronounced (see also Table 1) for the different authors. We therefore carried out a systematic study of the dependence of the zirconium tracer diffusion on the yttria content within a fairly wide range of stabilizer concentration (8...32 mol% Y_2O_3).

* Corresponding author.
E-mail address: martin.kilo@tu-clausthal.de (M. Kilo).

PII: S0955-2219(00)00072-8

Table 1
Experimental values of the zirconium tracer diffusivities obtained by different methods and the parameter **m** and **ΔH** (see text)[a]

	$[Y_2O_3]$	$[Y'_{Zr}]$	D_0 ($cm^2\ s^{-1}$)	**ΔH** (eV)	Temperature range (°C)	Method	**m**
This work	0.08	0.148	0.033	4.5±0.2	1125–1460	^{96}Zr/SIMS	$(\partial \ln D_{Zr}/\partial \ln [Y'_{Zr}])_T$
See also	0.103	0.187	0.062	4.6±0.2	1125–1460	tracer diffusion	$=-1.95\pm0.20$
Kilo et al.[10]	0.124	0.221	0.0083	4.4±0.2	1125–1460		
	0.156	0.270	0.094	4.8±0.2	1125–1460		
	0.186	0.313	0.021	4.6±0.5	1125–1460		
	0.24	0.387	0.0041	4.5±0.4	1125–1460		
	0.32	0.484	0.013	4.6±0.3	1125–1460		
Solmon[5]	0.095	0.173	0.33	4.95±0.05	1300–1700	^{96}Zr/SIMS	$(\partial \ln D_{Zr}/\partial \ln [Y'_{Zr}])_T$
See also	0.11	0.198	0.12	4.8±0.2	1300–1700	tracer diffusion	$=-2.6\pm0.2$
Solmon et al. [6]	0.177	0.301	0.066	4.93±0.05	1300–1700		
Gómez-García et al.[9]	0.094	0.172	–	6.1±0.3	$\geqslant$1500	Creep	$(\partial \ln D_{Zr}/\partial \ln [Y'_{Zr}])_T$
	0.12	0.214	–	5.6±0.5	$\geqslant$1500		$=(1+[Y_2O_3])$
	0.15	0.261	–	5.5±0.7	$\geqslant$1500		$\cdot(\partial \ln \dot{\varepsilon}/\partial \ln [Y_2O_3])_T$
	0.18	0.305	–	6.0±0.7	$\geqslant$1500		$=-(1.094\ ...\ 1.2)\cdot 3.2...$
	0.21	0.347	–	5.8±0.5	$\geqslant$1500		$\approx -3.5\ ...-3.8$
Chien and Heuer[7]	0.094	0.172	1.4	5.3±0.1	1100–1275	Dislocation loop	$(\partial \ln D_{Zr}/\partial \ln [Y'_{Zr}])_T$
	0.18	0.305	0.96	5.3±0.1	1100–1300	shrinkage	$=-4.7\pm0.4$
Dimos and Kohlstedt[8]	0.20	0.33	$3\cdot10^3$	5.85	1400–1600	Creep	–

[a] $\dot{\varepsilon}$, stationary creep rate at constant strain.

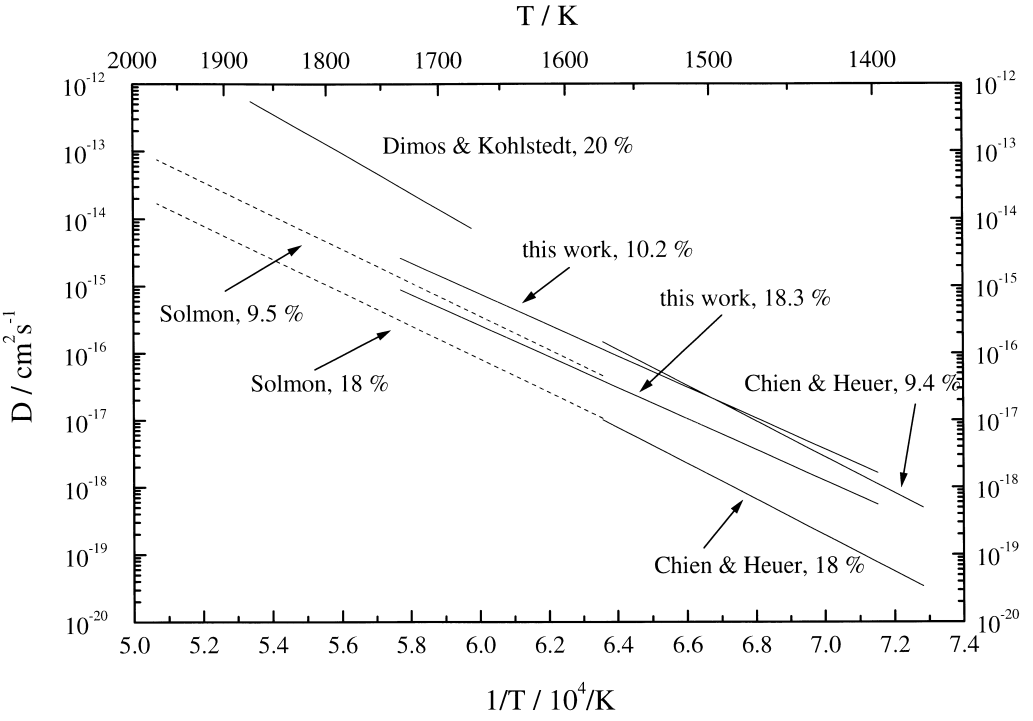

Fig. 1. Comparison of recent experimental data on cation diffusion in yttria stabilized zirconia (cf. Table 1).

In addition to the self-diffusion experiments, there is a wide range of diffusion experiments using different foreign cations in YSZ which will be mentioned for comparison:

- Manganese diffusion in YSZ with 10 mol% Y_2O_3: Kilner and co-workers[11] found rather high activation enthalpies for migration (7.3 eV). The authors explained their observations assuming that the oxidation state of the cations might have been changed during the diffusion experiment. The diffusion coefficients are higher by a factor of 10 than the self-diffusion data for Zr.
- Ti-diffusion in stabilized zirconia:[12] Kowalski et al. investigated the diffusion of titanium which has the same oxidation state as Zr, and hence no extra-vacancies should be formed in YSZ. The authors mentioned that their values are in good agreement

with data of Oishi et al.,[4] but did not discuss the obtained results in more detail.

- La-, Sr-, and Ni-diffusion in stabilized zirconia:[13] The diffusivities of these elements were checked in single crystalline YSZ. It was observed that the activation enthalpy of diffusion was lower for Sr^{2+} (4.2 eV) than for La^{3+} (5.0 eV).
- Calcium diffusion in stabilized zirconia containing 10 mol% Y_2O_3: Recently, Nowotny and co-workers[14] presented some data concerning the diffusion of Ca in polycrystalline YSZ. They found a fairly low activation enthalpy (about 4 eV) and surprisingly high diffusivities, several orders of magnitude higher than expected by extrapolating the scarce self-diffusion data. According to the authors, this might be influenced by the varying chemical potential gradient.

Finally, for comparison also some relevant data concerning the diffusion in related oxide systems should be mentioned. An overview of data and proposed mechanisms of diffusion in fluorite systems gives:[15]

- Chen and Chen[16] measured the grain boundary mobilities in ceria doped with different trivalent cations (Sc, Yb, Y, Gd, La). Therefrom, they determined grain boundary diffusion coefficients. The peculiarity of this system in comparison to YSZ is that the cubic fluorite phase is stable down to room temperature even in undoped pure CeO_2; the whole stabilizer concentration range is accessible without changes in the crystal structure. Consequently, the study emphasizes the low dopant concentration range 0.1 to 1.0% for which the authors proposed an interstitial mechanism for cation diffusion. In another publication,[17] the authors investigated the grain boundary mobility in Y_2O_3, also doped with a wide range of cations similar to Ref. 16. They suggested also that an interstitial mechanism should be predominant for the cation mobility and estimated a migration enthalpy of about 5 eV.
- Matzke[18,19] investigated the cation diffusion in the systems ThO_2, ThO_2–$UO_{2\pm\delta}$, and $UO_{2\pm\delta}$. The latter system is also cubic fluorite without stabilization, and with respect to the mechanism of cation diffusion it is especially interesting that both over- and under-stoichiometric uranium oxide are accessible. Matzke proposed a vacancy mechanism for stoichiometric and over-stoichiometric $UO_{2+\hat{O}}$, while for under-stoichiometric $UO_{2-\hat{O}}$, an interstitial mechanism should govern the self-diffusion of the cation. The activation enthalpies for cation diffusion are significantly different, 2.8 eV in $UO_{2+\delta}$, and 6.5 eV in $UO_{2-\delta}$

A major problem with ceria and urania is that they are generally easily reducible or oxidizible, so great care has to be taken in order to avoid any changes of the oxidation state during the diffusion experiment.

2. Point defect relations

In this section, the point defect equilibria are presented which lead to the working equations used in this paper to evaluate the available data. The relation between the point defect concentration and the experimentally determined tracer diffusivity D_i is based on the well established equation (1):

$$D_i = (c_{defect}/c_i)\cdot D_{defect}\cdot f \tag{1}$$

where D and c are diffusivities and concentrations, respectively. The subscript "i" refers to the (diffusing) species of interest, e.g. zirconium ions, whereas the subscript "defect" stands for the responsible defect, e.g. vacancies. The correlation factor f depends on the crystal structure and on the diffusion mechanism. While for a vacancy mechanism the contribution of the crystal structure is well known ($f\approx0.653$ for the fluorite lattice), the concentration dependence cannot easily be taken into account.[20] As will be seen from the relations developed below, a detailed knowledge of the fine structure is not necessary in order to elucidate the main features of the underlying cation transport processes.

Using Kröger–Vink notation the incorporation of yttria into zirconia and the related Schottky and Frenkel equilibria can be formulated (see below). The quantities [i] denote appropriately defined atomic fractions of the species i under consideration on the two sublattices. The quantities $K(T)$ are the "practical" mass action law constants for the respective reactions. The very few activity measurements of the two constituent binary oxide components in YSZ (Belov et al.[21,22] and Róg et al.[23]) and in calcia stabilized cubic zirconia (CSZ) (Róg et al.[24]) seem to indicate that such solutions can be treated as "ideal" to regular solutions. This statement does, of course, not shed direct light on the interaction thermodynamics of the cation point defects. For practical purposes, however, we do not commit a big error in considering the activity coefficients in the point defect equilibria as constant and in including them in the "practical" $K(T)$ terms.

- Incorporation of yttria

$$2Zr_{Zr}^{x} + O_{O}^{x} + Y_2O_3 \rightarrow 2Y'_{Zr} + V_{O}^{2\cdot} + 2ZrO_2 \tag{2a}$$

$$K_I = [Y'_{Zr}]^2[V_{O}^{2\cdot}] = \exp(-\Delta G_I/k_BT) \tag{2b}$$

- Schottky equilibrium:

Zr sites occupied by Zr_{Zr}^{x} ions:

$$Zr_{Zr}^{x} + 2\,O_{O}^{x} \rightarrow V_{Zr}^{4'} + 2\,V_{O}^{2\cdot} + ZrO_2 \tag{3a}$$

$$K_{S,Zr} = \left[V_{Zr}^{4'}\right]\cdot\left[V_{O}^{2\cdot}\right]^2 = \exp\left(-\Delta G_{S,Zr}/k_B T\right) \tag{3b}$$

Zr sites occupied by Y'_{Zr} ions:

$$2\,Y'_{Zr} + 3\,O_{O}^{x} \rightarrow 2\,V_{Zr}^{4'} + 3\,V_{O}^{2\cdot} + Y_2O_3 \tag{4a}$$

$$K_{S,Y} = \left[V'_{Zr}\right]^2\cdot\left[V_{O}^{2\cdot}\right]^3 = \exp\left(\Delta G_{S,Y}/k_B T\right) \tag{4b}$$

- Frenkel equilibrium

Zr sites occupied by Zr_{Zr}^{x} ions:

$$Zr_{Zr}^{x} \rightarrow V_{Zr}^{4'} + Zr_{i}^{4\cdot} \tag{5a}$$

$$K_{F,Zr} = \left[V_{Zr}^{4'}\right]\cdot\left[Zr_{i}^{4\cdot}\right] = \exp\left(-\Delta G_{F,Zr}/k_B T\right) \tag{5b}$$

Zr sites occupied by Y'_{Zr} ions:

$$Y'_{Zr} \rightarrow V_{Zr}^{4'} + Y_{i}^{3\cdot} \tag{6a}$$

$$K_{F,Y} = \left[V_{Zr}^{4'}\right]\cdot\left[Y_{i}^{3\cdot}\right] = \exp\left(-\Delta G_{F,Y}/k_B T\right) \tag{6b}$$

- Electroneutrality condition

The overall electroneutrality condition (ENC), (7a), expressed with total concentrations $\{i\}$ in cm^{-3}, can be written in a simplified form because of the dominating concentration of free, i.e. unbound, majority defects:

$$\begin{aligned} &2\left\{V_{O}^{2\cdot}\right\} + 4\left\{Zr_{i}^{4\cdot}\right\} + 3\left\{Y_{i}^{3\cdot}\right\} + \left\{\left(Y'_{Zr}V_{O}^{2\cdot}\right)^{\cdot}\right\} \approx 2\left\{V_{O}^{2\cdot}\right\} \\ &\rightarrow\ 2\left\{V_{Zr}^{4'}V_{O}^{2\cdot}\right\}^{2'} + \left\{Y'_{Zr}\right\} + 4\left\{V'_{Zr}\right\} + 2\left\{O_{i}^{2'}\right\} \approx \left\{Y'_{Zr}\right\} \end{aligned} \tag{7a}$$

Expressed as atomic fractions on the two respective sublattices, Eq. (7a) yields

$$\left[V_{O}^{2\cdot}\right] \approx \left[Y'_{Zr}\right]/4 \tag{7b}$$

which will be used in future.

Because of the high concentration of the majority point defects $V_{O}^{2\cdot}$ and Y'_{Zr}, defect complexes are highly probable to be formed. As suggested by Chien and Heuer[7] on the basis of their calculations, $Zr_{Zr}^{4\cdot}$ interstitials do not contribute to Zr migration, neither as an isolated defect nor as part of a complex defect. On the contrary, two cation vacancy containing complexes labelled A1 and A2 in the following might play a role:

- Complex A1

$$V_{Zr}^{4'} + V_{O}^{2\cdot} \rightarrow \left(V_{Zr}^{4'}V_{O}^{2\cdot}\right)^{2'} \tag{8a}$$

$$\begin{aligned} K_{A1,Zr} &= \left[\left(V_{Zr}^{4'}V_{O}^{2\cdot}\right)^{2'}\right]/\left(\left[V_{Zr}^{4'}\right]\cdot\left[V_{O}^{2\cdot}\right]\right) \\ &= \exp(-\Delta G_{A1}/k_B T) \end{aligned} \tag{8b}$$

$$K_{A1,Zr} = \left[\left(V_{Zr}^{4'}V_{O}^{2\cdot}\right)^{2'}\right]\cdot\left[V_{O}^{2\cdot}\right]/K_{S,Zr} \quad \text{[from Eq. (8b) with Eq. (3b)]} \tag{8c}$$

$$K_{A1,Zr} = \left[\left(V_{Zr}^{4'}V_{O}^{2\cdot}\right)^{2'}\right]\cdot\left[Y'_{Zr}\right]/\left(4\cdot K_{S,Zr}\right) \quad \text{[from Eq. (8c) with Eq. (7b)]} \tag{8d}$$

$$K_{A1,Y} = \left[\left(V_{Zr}^{4'}V_{O}^{2\cdot}\right)^{2'}\right]\cdot\left[Y'_{Zr}\right]^{1/2}/\left(2\cdot K_{S,Y}^{1/2}\right) \quad \text{[from Eq. (8c) with Eqs. (4b) and (7b)]} \tag{8e}$$

- Complex A2

$$V_{Zr}^{4'} + 2\,V_{O}^{2\cdot} \rightarrow \left(V_{Zr}^{4'}2V_{O}^{2\cdot}\right)^{x} \tag{9a}$$

$$K_{A2,Zr} = \left[\left(V_{Zr}^{4'}2V_{O}^{2\cdot}\right)^{x}\right]/K_{S,Zr} \quad \text{[from Eq. (9a) with Eq. (3b)]} \tag{9b}$$

$$K_{A2,Y} = 2\cdot\left[\left(V_{Zr}^{4'}2V_{O}^{2\cdot}\right)^{x}\right]/\left(\left[Y'_{Zr}\right]^{1/2}K_{S,Y}^{1/2}\right) \quad \text{[from Eq. (9a) with Eqs (4b) and (7b)]} \tag{9c}$$

Neglecting correlation effects, a tracer diffusivity can be expressed as the product of the defect concentration and an exponential term containing the migration enthalpy of diffusion, $\Delta H_{m,defect}$, where the second right bottom subscript indicates the defect via which diffusion occurs. Starting with the least probable case the following relation between the diffusivity of Zr and the molar fraction of the dopant $\left[Y'_{Zr}\right]$ can be derived.

- Interstitial mechanism

With $K_{S,Zr}$, $K_{F,Zr}$ and ENC from Eqs. (3b), (5b) and (7b), respectively, we get:

$$D_{Zr,i} = D_{Zr} \propto \left[Zr_{i}^{4\cdot}\right]\exp\left(-\Delta H_{m,i}/k_B T\right) \tag{10a}$$

$$\propto \left[V_{Zr}^{4'}\right]^{-1}K_{F,Zr}\exp\left(-\Delta H_{m,i}/k_B T\right) \tag{10b}$$

$$\propto \left[Y'_{Zr}\right]^2\left(K_{F,Zr}/16K_{S,Zr}\right)\exp\left(-\Delta H_{m,i}/k_B T\right) \tag{10c}$$

$$\propto \left[Y'_{Zr}\right]^2\exp\left(-\left(\Delta H_{m,i} + \Delta H_{F,Zr} - \Delta H_{S,Zr}\right)k_B T\right) \tag{10d}$$

Using Eq. (4b) instead of Eq. (3b) we arrive at the following expression

$$D_{Zr,i} = D_{Zr} \propto \left[Y'_{Zr}\right]^{3/2} \exp\left(-(\Delta H_{m,i} + \Delta H_{F,Zr} - \Delta H_{S,Y}/2)/k_B T\right) \quad (10e)$$

- Vacancy mechanism

With $K_{S,Zr}$ and ENC from Eqs. (3b) and (7b) we get:

$$D_{Zr,V} = D_{Zr} \propto \left[V''_{Zr}\right] \exp\left(-\Delta H_{m,V}/k_B T\right) \quad (11a)$$

$$\propto \left[V^{2\cdot}_{O}\right]^{-2} K_{S,Zr} \exp\left(-\Delta H_{m,V}/k_B T\right) \quad (11b)$$

$$\propto \left[Y'_{Zr}\right]^{-2} \exp\left(-\left(\Delta H_{m,V} + \Delta H_{S,Zr}\right)/k_B T\right) \quad (11c)$$

With $K_{Y,Zr}$ and ENC from Eqs. (4b) and (7b) follows:

$$D_{Zr,V} = D_{Zr} \propto \left[V^{2\cdot}_{O}\right]^{-3/2} K^{1/2}_{S,Y} \exp\left(-\Delta H_{m,V}/k_B T\right) \quad (11d)$$

$$\propto \left[Y'_{Zr}\right]^{-3/2} \exp\left(-\left(\Delta H_{m,V} + \Delta H_{S,Y}/2\right)k_B T\right) \quad (11e)$$

- Diffusion via A1 complex $\left(V''_{Zr}V^{2\cdot}_{O}\right)^{2'}$

With $K_{S,Zr}$, K_{A1} and ENC from Eqs. (3b), (8d) and (7b) follows:

$$D_{Zr,A1,Zr} = D_{Zr} \propto \left[\left(V''_{Zr}V^{2\cdot}_{O}\right)^{2'}\right] \exp\left(-\Delta H_{m,A1,Zr}/k_B T\right) \quad (12a)$$

$$\propto \left[Y'_{Zr}\right]^{-1} 4 \cdot K_{S,Zr} \cdot K_{A1,Zr} \cdot \exp\left(-\Delta H_{m,A1,Zr}/k_B T\right) \quad (12b)$$

$$\propto \left[Y'_{Zr}\right]^{-1} \cdot \exp\left(-\left(\Delta H_{m,A1,Zr} + \Delta H_{S,Zr} + \Delta H_{A1,Zr}\right)/k_B T\right) \quad (12c)$$

With $K_{S,Y}$ from Eq. (4b) instead of Eq. (3b) we get:

$$D_{Zr,A1,Y} = D_{Zr} \propto \left[Y'_{Zr}\right]^{-1/2} \exp\left(-\left(\Delta H_{m,A1,Y} + \Delta H_{S,Y}/2 + \Delta H_{A1,Y}\right)/k_B T\right) \quad (12d)$$

- Diffusion via A2 complex $\left(V''_{Zr}2V^{2\cdot}_{O}\right)^{x}$

With $K_{S,Zr}$, K_{A2} and ENC from Eqs. (3b), (9b) and (7b) follows:

$$D_{Zr,A2,Zr} = D_{Zr} \propto \left[\left(V''_{Zr}2V^{2\cdot}_{O}\right)^{x}\right] \exp\left(-\Delta H_{m,A2,Zr}/k_B T\right) \quad (13a)$$

$$\propto K_{S,Zr} \cdot K_{A2,Zr} \cdot \exp\left(-\Delta H_{m,A2,Zr}/k_B T\right) \quad (13b)$$

$$\propto \exp\left(-\left(\Delta H_{m,A2,Zr} + \Delta H_{S,Zr} + \Delta H_{A2,Zr}\right)/k_B T\right) \neq f\left(\left[Y'_{Zr}\right]\right) \quad (13c)$$

In order to rationalize the experimental observations in Table 1 we define the quantities

$$\partial \ln D_{Zr}/\partial \ln\left[Y'_{Zr}\right] =: \mathbf{m} \quad (14)$$

$$-k_B \cdot \partial \ln D_{Zr}/\partial(1/T) =: \mathbf{\Delta H} \quad (15)$$

which permits to identify the Zr diffusion mechanism, as can be inferred from Table 2. For the data compilation given in Table 1 the following relations were used in order to get all the data in the same format:

$$\mathbf{m} := \partial \ln D_{Zr}/\partial \ln\left[Y'_{Zr}\right] = \frac{(\partial \ln D_{Zr}/\partial \ln[Y_2O_3])}{\left(\partial \ln\left[Y'_{Zr}\right]/\partial \ln[Y_2O_3]\right)} = (\partial \ln D_{Zr}/\partial \ln[Y_2O_3]) \cdot (1 + [Y_2O_3]) \quad (16)$$

because

$$\left[Y'_{Zr}\right] = 2[Y_2O_3]/(1 + [Y_2O_3]) \quad (17)$$

which is equivalent to the concentration variable x in the relation $Zr_{1-x}Y_xO_{2-x/2}$.

3. Experimental procedure

3.1. Samples

Y_2O_3–ZrO_2 single crystal samples were obtained from Zirmat Corporation, North Billerica, USA. Samples with nominal stabilizer concentrations of 10, 12, 15, 18, 24, and 32 mol% Y_2O_3 were investigated. The compositions were checked by standard chemical analysis at the Max-Planck-Institut für Metallforschung, Stuttgart. Particle induced X-ray emission spectroscopy (PIXE)

Table 2
m and **ΔH** values as defined by Eqs. (14) and (15) for typical defects likely to assure Zr diffusion (see text)

Defect	**m**	**ΔH**	From Eq.
$Zr^{4\cdot}_i$	2	$\Delta H_{m,i} + \Delta H_{F,Zr} - \Delta H_{S,Zr}$	(10d)
$Zr^{4\cdot}_i$	1.5	$\Delta H_{m,i} + \Delta H_{F,Zr} - \Delta H_{S,Y}/2$	(10e)
V''_{Zr}	−2	$\Delta H_{m,V+} \Delta H_{S,Zr}$	(11c)
V''_{Zr}	−1.5	$\Delta H_{m,V+} \Delta H_{S,Y}/2$	(11e)
$(V''_{Zr}\ V^{2\cdot}_{O})^{2'}$	−1	$\Delta H_{m,A1,Zr} + \Delta H_{S,Zr} + \Delta H_{A1,Zr}$	(12c)
$(V''_{Zr}\ V^{2\cdot}_{O})^{2'}$	−0.5	$\Delta H_{m,A1,Y} + \Delta H_{S,Y}/2 + \Delta H_{A1,Y}$	(12d)
$(V''_{Zr}\ 2V^{2\cdot}_{O})^{x}$	0	$\Delta H_{m,A2,Zr} + \Delta H_{S,Zr} + \Delta H_{A2,Zr}$	(13c)

was used to determine cation impurities showing predominantly alkali and alkaline earth metals with altogether less than 0.1%. The composition of the investigated samples is given in Table 3, including the atomic fraction of yttrium ions on the sublattice, $[Y_{Zr}']$, which is proportional to the (formal) total concentration of oxygen vacancies [see Eq. (7b)], but is not linearly proportional to the yttria content, $[Y_2O_3]$ [see Eq. (17)]. Furthermore, a high purity polycrystalline sample containing 8 mol% yttria was also investigated. This material has been fabricated by Professor Schubert's group at Technische Universität Berlin in a binder-free route from a powder manufactured by Tosoh Corporation, Japan. Uniaxial compaction (pressure 20 MPa) at room temperature was followed by isostatic compaction (300 MPa) prior to sintering at 1680 °C for 2 h in air. The heating and cooling rates were 1 and 3 K/min, respectively.

3.2. Preparation

The samples were cut into slabs of ca. $10\times10\times1$ mm^3 size and polished with an alumina suspension (''Final'', particle size: 500 nm). Thereafter, the specimens were annealed for 2 days at 1460 °C in air.

3.3. Isotopic labelling

^{96}Zr was implanted from zirconium chloride having natural isotopic abundance. The metal was ionized, the isotope separated and a dose of $6\cdot10^{15}$ ions/cm^2 was implanted using a primary energy of 150 keV. The observed implantation depth was 36 nm. Furthermore, ^{96}Zr was obtained from Chemotrade GmbH, Düsseldorf, Germany, as zirconium dioxide, containing 59.6% ^{96}Zr (natural isotopic abundance: 2.8%). The oxide was dissolved in HF, evaporated, dissolved again in HNO_3, and diluted with ethanol. Small amounts of this solution (also containing a respective amount of $Y(NO_3)_3$) were dropped repeatedly onto the substrates and dried at 100 °C. In this way, thin films of less than 50 nm nominal thickness were obtained having no chemical gradient.

Table 3
Composition of the investigated yttria stabilized zirconia samples

Sample label	$x(Y_2O_3)$ (mol%)	x(Y) (mol%)	Checked
Y8	7.8	14.5	[a]
Y10	10.2	18.5	[a]
Y12	12.4	22.1	[a]
Y15	15.6	27.0	[a]
Y18	18.6	31.4	[b]
Y24	24.0	38.7	[b]
Y32	32.1	48.5	[a]

[a] Checked by chemical analysis.
[b] Checked by PIXE.

3.4. SIMS experiments

For the SIMS depth profile analysis a VG SIMS-Lab was used. Cs^+ or Ar^+ primary ions, respectively, with an energy of 8 keV were scanned over a sample area of about 1×1 mm^2. Singly charged secondary ions (cations) were detected. An electronic gating of 30% in each direction was applied to reduce crater rim effects. To avoid sample charging a flood gun was used. To convert sputter time into eroded depth the crater depth was measured using a profilometer (Tencor). The SIMS technique has an ultimate depth resolution of several nm, which is significantly better than for standard radiotracer sectioning techniques. Therefore, lower diffusion temperatures are accessible and erroneous confusion of self diffusion and grain-boundary diffusion as observed earlier in UO_2[18,19] can be easily avoided. Furthermore, for selected experiments repeated at different annealing times no time dependency of the cation diffusion coefficient was observed. In a previous study on the diffusion of foreign cations,[13] diffusion along dislocations and in the bulk was observed which could be easily separated according to standard recipes.[25] It came out that the latter contributes significantly to the measured SIMS signal only at high penetration depth. In this study similar experimental conditions were applied. Applying the quoted evaluation procedure[25] to the experimentally determined penetration profiles clearly shows that transport along dislocations can be neglected.

Therefore, bulk tracer diffusivities D are calculated by fitting the appropriate solution of Fick's second law[26] to the tracer isotope concentration profile. Eq. (18) describes the profiles to a fully satisfactory precision (see also Fig. 2):

$$c(x,t)-c_0 = 0.5\cdot(c_s-c_0)\cdot\left(\mathrm{erf}\left((x+h)/2(Dt)^{0.5}\right)-\mathrm{erf}\left((x-h)/2(Dt)^{0.5}\right)\right) \quad (18)$$

where c_0 and c_s are the natural abundance and the initial concentration of the tracer isotope, respectively, h is the thickness of the tracer layer, x is the depth and t the diffusion time. All tracer diffusivities obtained were analysed as to their temperature and concentration dependence as described in Section 2. As an example for the concentration dependency, we refer to Fig. 3. The obtained data (D_0, $\Delta\mathbf{H}$) are given in Table 1 as well as the resulting mean value of the concentration parameter **m** ($=-1.95\pm0.2$).

4. Discussion

In Section 2, the point defect chemistry based relations necessary to interpret the experiments in Table 1

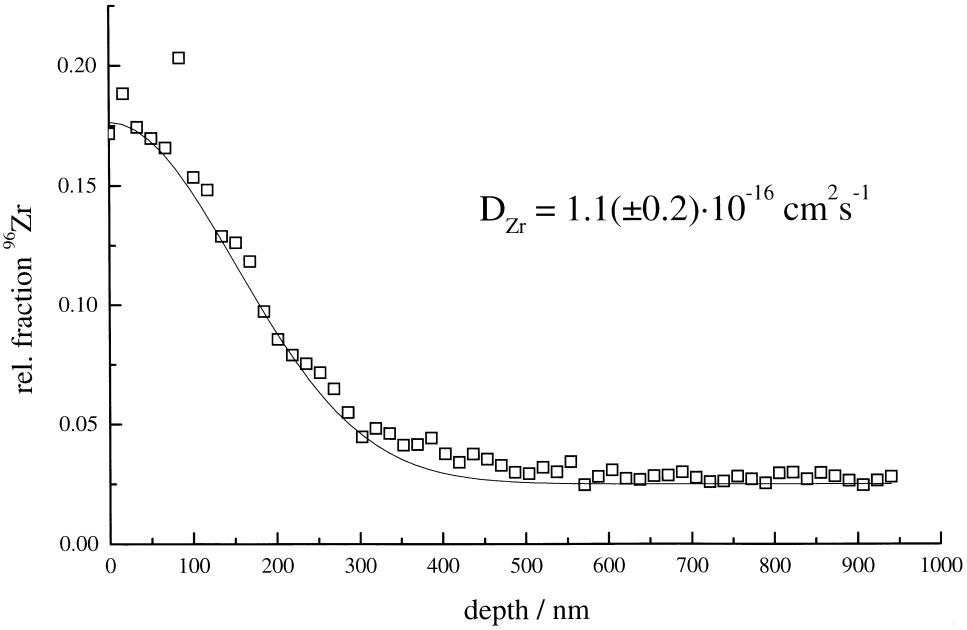

Fig. 2. ^{96}Zr depth profile of the sample ZrO_2(18.6 mol% Y_2O_3) after diffusion at 1350°C for 270 h.

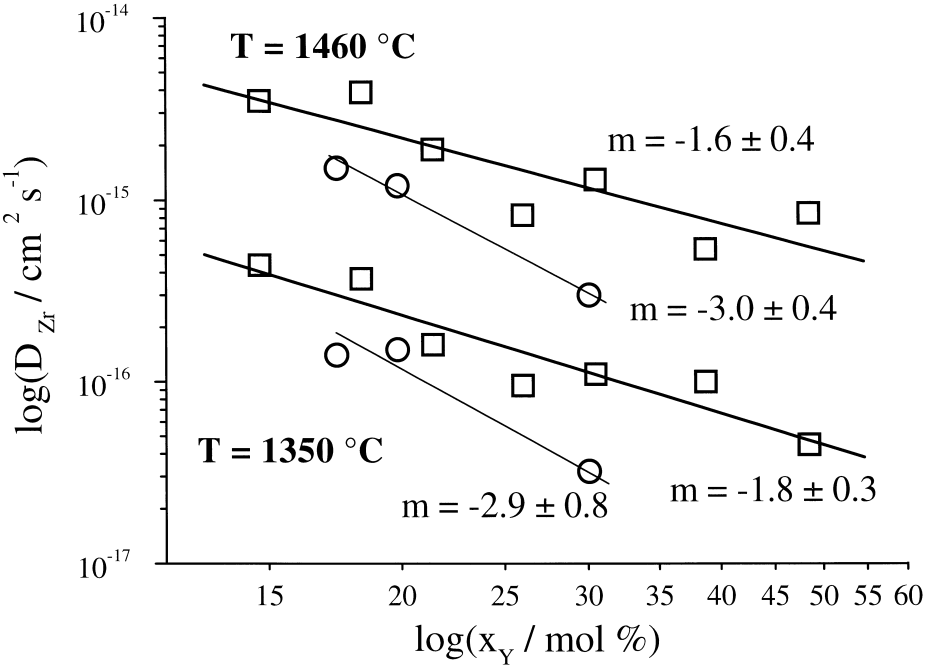

Fig. 3. Concentration dependence of the zirconium tracer diffusion at the indicated temperatures. Squares: our data; circles: results of Solmon.[6] The respective values of the parameter **m** are shown (see text).

have been developed. The resulting working Eq. (14) and the **m** values calculated from the data are given in the right-hand column of Table 1. Whereas for our own work and the data published by Chien and Heuer,[7] Solmon et al.[5] and Solmon[6] the procedure is straightforward (including a recalculation of Solmon's data from her raw data[6]), we had to take the concentration dependence of the creep rate from Gómez-García et al.[9] as the authors did not calculate diffusivities themselves and only globally discussed the relation between creep rate and cation diffusion. As can be seen by comparing Table 2 and the experimental **m** values of -1.95 ± 0.2, the migration of cations via interstitials or via a complex defect can be discarded. The tracer diffusion based work (Solmon[5,6] and our own results) indicate a simple vacancy mechanism via free vacancies, V'''_{Zr}, excluding

the vacancy complexes $(V''_{Zr}\ V^{\cdot\cdot}_{O})^{\prime}$ and $(V''_{Zr}\ 2V^{\cdot\cdot}_{O})^{x}$ which were proposed by Chien and Heuer[7] from estimations of point defect concentrations based on computer simulation values for binding enthalpies.[27] In any case, the high absolute value for the parameter **m** for the dislocation loop shrinkage data (−4.7±0.4) and the creep data (−3.5 . . .−3.8) cannot be explained by taking any point defect complexes into account, as defect complex formation would lead to considerably lower absolute values of **m**.

According to Table 1, the experimental values of the activation enthalpy $\Delta\mathbf{H}$, which were determined through three different experimental techniques, are centred around 5 eV with a spread of less than 1 eV (see also the data collected by Jiménez-Melendo et al.[28] in their recent comprehensive article on superplastic flow in fine-grained tetragonal YSZ materials). This is far less than any value which could be calculated with the aid of the expressions given in Table 2 on the basis of computer simulation data of Mackrodt and Woodrow[27] or Dwivedi and Cormack.[29] As an example, we take Eq. (11c) in Table 2 which would yield $\Delta\mathbf{H} = (11.6 + 8.5)$ eV $\approx$20 eV if the calculated values were used (see Tables II and V in Ref. 27 for lattice defect energies for the Schottky triple defect and for migration enthalpies).

From a pragmatic point of view, it is difficult to envisage the independent experimental verification of a Schottky formation enthalpy of more than about 3 to 4 eV. Moreover, in analogy to cation diffusion in other oxide structures (see overview of Catlow et al.,[30] Table VII for α-Fe_2O_3, α-Cr_2O_3 and α-Al_2O_3) realistic values for the cation vacancy migration enthalpy $\Delta H_{m,V}$ should be between 2 and 3 eV. On the other hand, Chen and Chen[16] claimed for CeO_2 that cation diffusion occurs via an interstitial mechanism, similar to Matzke,[18] who proposed the same mechanism for the UO_2 system. Both authors gave for the fluorite systems values of 5 eV for the migration enthalpies in doped fluorites. It should be noted that they only investigated samples with dopant levels or non-stoichiometry of virtually 0–3%. In contrast to these systems whose properties might be partly influenced by intrinsic defects, the investigated YSZ is extrinsic over the whole concentration range. It might be also interesting to note that we recently observed in CSZ doped with 10 to 17 mol% CaO similar values of the activation enthalpies for cation transport[31] (5. . .5.5 eV).

As to the major discrepancies between the experimental values and the calculated values of the activation enthalpies, we propose a recalculation of the theoretical values, since recently big progress in computer modelling of solids has been achieved.

It is difficult to explain the minor difference between the enthalpy data obtained from direct diffusion measurements, which are about 1 eV lower as compared to the data extracted from creep and dislocation loop shrinking experiments. One reason might be an appreciable difference between the diffusivity of zirconium and of yttrium if the latter one were the rate determining species. On the other hand, such a difference should lead to kinetic demixing which was not observed as yet.[8] Furthermore, by a very indirect way, Solmon[5,6] concluded that yttrium diffusion is at best four times faster than zirconium diffusion.

5. Conclusions

Based on a joint evaluation of tracer diffusion data, dislocation loop shrinkage data and creep data it is concluded that Zr self-diffusion in YSZ most probably occurs via a single vacancy mechanism, i.e. via the point defect V''_{Zr}. While there is substantial agreement between our data and the published values of the activation enthalpies there is no agreement between the experimental values and published calculated data for the activation enthalpies.

Acknowledgements

We gratefully appreciate substantial help with the sample preparation and most valuable discussions offered by M. Weller, A. Lakkis, C. Reetz, H. Schubert, and E. Ebeling. H.-D. Carstanjen and N. Pazarkas kindly carried out PIXE analyses. Financial support from the Deutsche Forschungsgemeinschaft (DFG) made this work possible. One of the authors (S.W.) is especially indebted to the TMR Programme of the EU for financial assistance via the COPES Large Scale Facility at TU Clausthal. An anonymous referee helped to improve the clarity of the manuscript.

References

1. Stubican, V. S., Corman, G. S., Hellman, J. R. and Senft, G., Phase relationships in some ZrO_2 systems. In *Adv. Ceram.: Science and Technology of Zirconia 2*, Vol. 12, ed. N. Claussen, M. Rühle and A. H. Heuer. The American Ceramic Society, Columbus, OH, 1983, pp. 96–106.
2. Kilner, J. A. and Brook, R. J., A study of oxygen ion conductivity in doped non-stoichiometric oxides. *Solid State Ionics*, 1982, **6**, 237–252.
3. Kondoh, J. et al., Effect of aging on yttria-stabilized zirconia. *J. Electrochem. Soc.*, 1998, **145**, I: 1527–1536; II: 1536–1550; III: 1550–1560.
4. Oishi, Y., Ando, K. and Sakka, Y. Lattice and grain-boundary diffusion coefficients of cations in stabilized zirconias. In *Adv. Ceram.: Additives and Interfaces in Electronic Ceramics* Vol. 7 ed. M. F. Yan and A. H. Heuer. The American Ceramic Society, Columbus, OH, 1983, pp. 208–219.
5. Solmon, H., Chaumont, J., Dolin, C. and Monty, C., Y, Zr, and O self diffusion in $Zr_{1-x}Y_xO_{2-x/2}$ ($x = 0.17$). *Ceram. Trans.*, 1991, **24**, 175–184.

6. Solmon, H., Autodiffusion de l'oxygène, du zirconium et de l'yttrium dans la zircone cubique stabilisée par l'yttrium, Ph.D. thesis, Université Paris 6, 1992.
7. Chien, F. R. and Heuer, A. H., Lattice diffusion kinetics in Y_2O_3-stabilized cubic ZrO_2 single crystals: a dislocation loop annealing study. *Philos. Mag. A*, 1996, **73**, 681–697.
8. Dimos, D. and Kohlstedt, D. L., Diffusional creep and kinetic demixing in yttria-stabilized zirconia. *J. Am. Ceram. Soc.*, 1987, **70**, 531–536.
9. Gómez-García, D., Martínez-Fernández, J., Domínguez-Rodríguez, A. and Castaing, J., Mechanisms of high-temperature creep of fully stabilized zirconia single crystals as a function of the yttria content. *J. Am. Ceram. Soc.*, 1997, **80**, 1668–1672.
10. Kilo, M., Borchardt, G., Weber, S., Scherrer, S. and Tinschert, K., Zirconium and calcium tracer diffusion in stabilized cubic zirconia. *Ber. Bunsen-Ges. Phys. Chem.*, 1997, **101**, 1361–1365.
11. Waller, D., Sirman, J. D. and Kilner, J. A., Manganese diffusion in single crystal and polycrystalline yttria stabilized zirconia. In *Proc. Electrochem. Soc.: Electrode Materials and Processes for Energy Conversion and Storage IV* Vol 97-18, ed. J. McBreen et al. The Electrochemical Society, Pennington, USA, 1997, pp. 1140–1149.
12. Kowalski, K., Bernasik, A., Sadowski, A., Janowski, J., Radecka, M. and Jedliński, J., SIMS investigation of titanium diffusion in yttria stabilized zirconia. In *Proceedings of ECASIA 7*, ed. I. Olefjord, L. Nyborg and D. Briggs. Wiley, Chichester, 1997, pp. 259–262.
13. Kilo, M., Borchardt, G., De Souza, R. A., Ivers-Tiffée, E., Weber, S. and Scherrer, S., Diffusion of foreign cations in stabilized zirconia. In *Proc. Electrochem. Soc.: Solid State Ionic Devices* Vol. 99-13, ed. E. D. Wachsman, J. R. Akridge, M. Liu and N. Yamazoe. The Electrochemical Society, Pennington, USA, 1999, pp. 228–237.
14. Matsuda, M., Nowotny, J., Thang, Z. and Sorrell, C. C., Lattice and grain boundary diffusion of Ca in polycrystalline yttria-stabilized ZrO_2 determined by employing SIMS technique. *Solid State Ionics*, 1998, **111**, 301–306.
15. Atkinson, A., Diffusion along grain boundaries and dislocations in oxides, alkali halides and carbides. *Solid State Ionics*, 1984, **12**, 309–320.
16. Chen, P.-L. and Chen, I.-W., Role of defect interaction in boundary mobility and cation diffusivity of CeO_2. *J. Am. Ceram. Soc.*, 1994, **77**, 2289–2297.
17. Chen, P.-L. and Chen, I.-W., Grain boundary mobility in Y_2O_3: defect mechanism and dopant effects. *J. Am. Ceram. Soc.*, 1996, **79**, 1801–1809.
18. Matzke, Hj., Lattice disorder and metal self-diffusion in non-stoichiometric UO_2 and $(U,Pu)O_2$. *J. Phys. (Paris) C*, 1973, **34**, 317–325.
19. Matzke, Hj., Diffusion of Th and U in thorium dioxide. *J. Phys. (Paris) C*, 1976, **37**, 452–457.
20. Murch, G. E., Ionic transport and tracer diffusion in a lattice containing random traps. *J. Phys. Chem. Solids*, 1985, **46**, 53–59.
21. Belov, A. N and Semenov, G. A., Mass spectrometric study of the evaporation of ZrO_2–HfO_2 ZrO_2–Y_2O_3. *Tugoplavkie Soedin. Redkozem. Met. (Mater. Vses. Semin.)*, 1979, **3**, 135–139.
22. Belov, A. N., Lopatin, S. I. and Semenov, G. A., Mass spectrometric study of the incongruent step in the evaporation of Lu_2O_3 and of ZrO_2–Y_2O_3 and ZrO_2-Lu_2O_3 solid solutions. *Russ. J. Phys. Chem. (Transl. Of Zh. Fiz. Khim.)*, 1981, **55**, 524–528.
23. Róg, G., Kozłowska-Róg, A., Haberko, K. and Bućko, M. M., Termodynamiczne własności roztworow stałych tworzących się w układach Me_pO_q-ZrO_2 (Me = Ca, Y, Ti). *Szkło Ceram.*, 1994, **45**, 1–4.
24. Róg, G., Haberko, K., Kozłowska-Róg, A. and Borchardt, G., Determination of CaO activity in the mixture $\{x\mathrm{CaO} + (1-x)\mathrm{ZrO_2}\}$ at the temperature K by a galvanic cell involving calcium-ion conducting solid electrolyte. *J. Chem. Thermodyn.*, 1995, **27**, 741–744.
25. Kaur, I., Mishin, Y. and Gust, W., *Fundamentals of Grain and Interphase Boundary Diffusion*, 3rd revised enlarged edn. J. Wiley & Sons Ltd, Chichester, 1995, pp. 222–243.
26. Crank, J., *The Mathematics of Diffusion*. Oxford University Press, Oxford, 1957 11-13.
27. Mackrodt, W. C. and Woodrow, P. M., Theoretical estimates of point defect energies in cubic zirconia. *J. Am. Ceram. Soc.*, 1986, **69**, 277–280.
28. Jiménez-Melendo, M., Domínguez-Rodríguez, A. and Bravo-León, A., Superplastic flow of fine-grained yttria-stabilized zirconia polycrystals: constitutive equation and deformation mechanism. *J. Am. Ceram. Soc.*, 1998, **81**, 2761–2776.
29. Dwivedi, A. and Cormack, A. N., A computer simulation study of the defect structure of calcia-stabilized zirconia. *Philos. Mag. A*, 1990, **61**, 1–22.
30. Catlow, C. R. A., Corish, J., Hennessy, J. and Mackrodt, W. C., Atomic simulation of defect structures and ion transport in α-Fe_2O_3 and α-Cr_2O_3. *J. Am. Ceram. Soc.*, 1988, **71**, 41–49.
31. Kilo, M., Borchardt, G., Weber, S., Scherrer, S., Tinschert, K., Lesage, B. and Kaïtasov, O., Cation diffusion in calcia stabilized zirconia (CSZ). *Radiat. Eff. Defects Solids*, 1999, **151**, 29–33.